Lifting Parameterisation of the 9/7 Wavelet Filter Bank and its Application in Lossless Image Compression

TILO STRUTZ
Deutsche Telekom AG, Hochschule für Telekommunikation
Institute of Communications Engineering
Gustav-Freytag-Str. 43-45, 04277 Leipzig
GERMANY
strutz@hft-leipzig.de

Abstract: The description of filter banks using lifting structures does not only benefit low-complexity implementation in software or hardware, but is also advantageous for the design of filter banks because of the guaranteed perfect reconstruction property. This paper proposes a new design method for wavelet filter banks, which is explained based on a single lifting structure suitable for 9/7 filter pairs. The modification of the standard design constraints leads to a family of related filter pairs with varying characteristics. The filters are derived directly, the factorisation of known filters is not necessary. The application of the designed filters to lossless image compression is investigated.

Key–Words: lifting scheme, filter design, wavelet transform, image coding

1 Introduction

Starting with the construction of the 9/7 wavelet filters for conventional two-channel filter banks, upon the first application in image compression [1] it became, within a family of wavelets [4], the most successful wavelet filter pair in lossy compression for a broad range of natural images such as photographs. This success was manifested in the compression standard JPEG2000 [7].

Daubechies and Sweldens [5] have shown that each two-channel filter bank consisting of filters with finite impulse response (FIR) can be implemented with the so-called lifting scheme, first introduced in [9]. The filter coefficients of single lifting steps can be determined via the factorisation of the polyphase matrix of the filter bank.

The description of filter banks using lifting structures leads to a distinct reduction in computational complexity and is especially attractive for filter design, since it guarantees perfect reconstruction of the filter bank to be constructed. This fact has inspired researchers, for example, to approximate the lifting coefficients of the well-known 9/7 wavelet filter bank by rational values for low-complexity hardware and software implementation [2, 6, 10] and to design similar 9/7 filter banks [11].

This contribution proposes a new design method directly yielding wavelet filter banks in lifting representation. No factorisation of known filter banks is required.

Apart from the abovementioned advantages of the lifting principle, it also enables the mapping of integer input samples to integer output samples, also known as integer wavelet transform (IWT) [3]. Integer transforms are a prerequisite when the application targets lossless image compression, for example.

The new design approach is explained using the 9/7 lifting representation as an example. Relaxing the constraints of the original filters from [4], the design can be parameterised leading to a family of related wavelet filters. The properties of these filters are analysed, their performance when applied to lossless image compression investigated and compared to the 5/3 wavelet filters used in JPEG2000.

The outline is as follows. The next section repeats the foundations of the lifting principle and introduces the flow chart used for the new approach. Section 3 explains the filter design, first with conventional constraints, followed by the parameterisation resulting in a family of related filter banks. Section 4 discusses the compression results and Section 5 summarises the article.

2 The lifting scheme

The conventional structure of two-channel filter banks based on lifting steps is shown in **Figure 1**. The incoming signal (z domain) is split into two paths (polyphase transform) containing the values at even or odd sample positions. In order to devise the filter

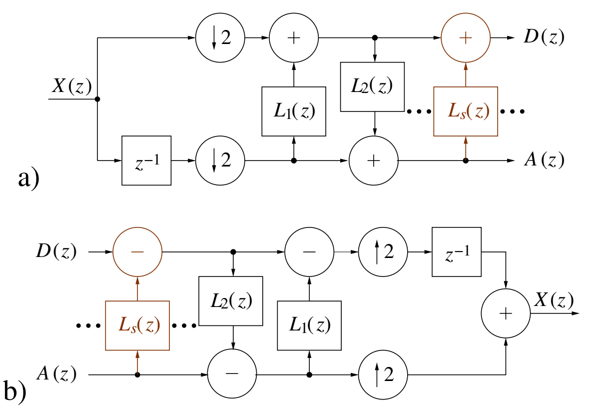

Figure 1: Principle of lifting with alternating steps: a) analysis, b) synthesis.

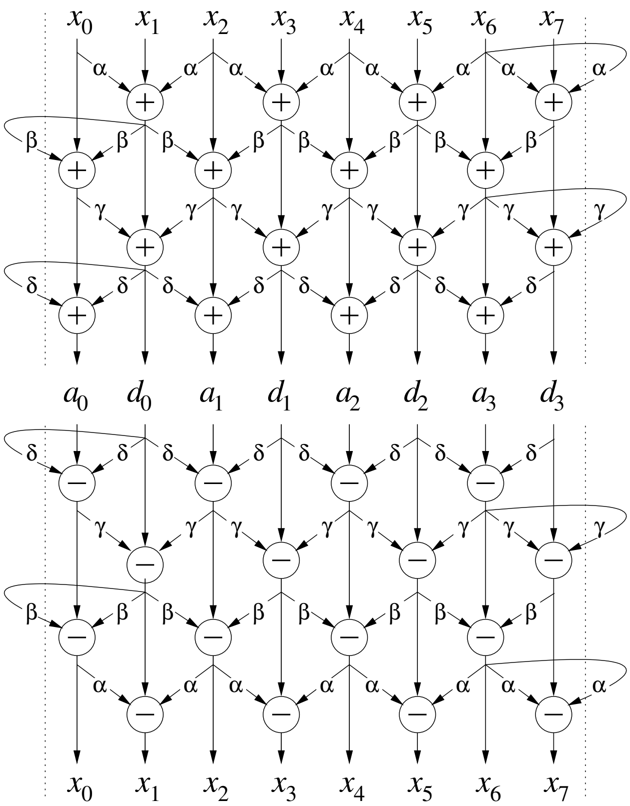

Figure 2: Signal flow in signal decomposition with 9/7-tap filters

properties, alternating lifting and dual lifting steps are applied, in which samples from one path are filtered by $L_i(z)$ and added to a sample of the other path.

With respect to the design method to be proposed, however, the illustration with a different flow chart is more helpful. **Figure 2** depicts a lifting cascade suitable for representing a 9-tap low-pass and a 7-tap high-pass filter pair. Essentially, it shows the signal flow for processing a signal with eight samples x_0 to x_7. A pair of samples at even positions is weighted by (typically negative) coefficients α and added to the sample in between. The next lifting step combines the results of the summations in pairs using the coefficients β. The third and fourth lifting step act in the same manner using the weights γ and δ.

The property of integer-to-integer mapping, which will be essential for lossless compression, is simply imposed by properly rounding the intermediate values to integer values [3] (not shown in the flow diagram).

The arithmetic calculations are (with $m = 0, 1, 2, \dots$)

$$\begin{aligned} d'_m &= x_{2m+1} + \lfloor \alpha\cdot(x_{2m} + x_{2m+2}) + 0.5 \rfloor \\ a'_m &= x_{2m} \quad + \lfloor \beta\cdot(d'_{m-1} + d'_m) + 0.5 \rfloor \\ d_m &= d'_m \quad + \lfloor \gamma\cdot(a'_m + a'_{m+1}) + 0.5 \rfloor \\ a_m &= a'_m \quad + \lfloor \delta\cdot(d_{m-1} + d_m) + 0.5 \rfloor \end{aligned} \tag{1}$$

The result after all lifting steps is an interleaved sequence of low-pass filter output a_m (approximation signal) and the high-pass filter output d_m (detail signal). Figure 2 also shows the reconstruction of the original signal x_n by performing the lifting steps in the reverse order and using the opposite signs

$$\begin{aligned} a'_m &= a_m - \lfloor \delta\cdot(d_{m-1} + d_m) + 0.5 \rfloor \\ d'_m &= d_m - \lfloor \gamma\cdot(a'_m + a'_{m+1}) + 0.5 \rfloor \\ x_{2m} &= a'_m - \lfloor \beta\cdot(d'_{m-1} + d'_m) + 0.5 \rfloor \\ x_{2m+1} &= d'_m - \lfloor \alpha\cdot(x_{2m} + x_{2m+2}) + 0.5 \rfloor\ . \end{aligned} \tag{2}$$

Furthermore, the flow diagram simply explains the exception handling at the signal borders. When applied to signals with an odd length, the handling has to be changed slightly.

3 Filter Design

3.1 Filters with maximum number of vanishing moments

The flow diagram, as depicted in Figure 2, allows the derivation of the analysis filters of the corresponding two-channel filter bank simply by considering all paths from the input samples to a particular approximation sample a_m or detail sample d_m, respectively. For the moment we will disregard the rounding operations. The resulting symmetric 7-tap impulse response of the analysis high-pass filter is

$$\begin{aligned} h_1[n] = \{\ & \alpha\beta\gamma \quad \beta\gamma \quad [\gamma\cdot(2\alpha\beta+1) + \alpha\cdot(1+\gamma\beta)] \\ & (2\beta\gamma+1) \quad [\gamma\cdot(2\alpha\beta+1) + \alpha\cdot(1+\gamma\beta)] \quad \beta\gamma \quad \alpha\beta\gamma\ \} \end{aligned} \tag{3}$$

and the analysis 9-tap low-pass filter reads as

$$\begin{aligned} h_0[n] = \{\ & \alpha\beta\gamma\delta \quad \beta\gamma\delta \\ & \{\delta\cdot[\gamma\cdot(2\alpha\beta+1) + \alpha\cdot(1+\gamma\beta)] + \alpha\beta\cdot(1+\gamma\delta)\} \end{aligned}$$

$$[\delta\cdot(2\beta\gamma+1)+\beta\cdot(1+\gamma\delta)]$$
$$\{\alpha\cdot[\delta\cdot(2\beta\gamma+1)+\beta\cdot(1+\gamma\delta)]+(1+2\gamma\delta)+$$
$$\alpha\cdot[\delta\cdot(2\beta\gamma+1)+\beta\cdot(1+\gamma\delta)]\}$$
$$[\delta\cdot(2\beta\gamma+1)+\beta\cdot(1+\gamma\delta)]$$
$$\{\delta\cdot[\gamma\cdot(2\alpha\beta+1)+\alpha\cdot(1+\gamma\beta)]+\alpha\beta\cdot(1+\gamma\delta)\}$$
$$\beta\gamma\delta \quad \alpha\beta\gamma\delta \quad \} \ . \tag{4}$$

The synthesis filters are derived by following all paths from a particular approximation (or detail) sample to the reconstructed signal values x_n. In this particular lifting structure, it turns out that they are directly related to the analysis filters by

$$g_0[n] = (-1)^{n+1}\cdot h_1[n] \quad n=0,1,2,\ldots \tag{5}$$
$$g_1[n] = (-1)^{n}\cdot h_0[n] \ . \tag{6}$$

The frequency response (in z-domain) of a t-tap filter $h[n]$ is

$$H(z)=\sum_{n=0}^{t-1} h[n]\cdot z^n \ . \tag{7}$$

Since $h_0[n]$ and $g_0[n]$ should be real low-pass filters, their magnitude responses at sampling frequency must be equal to zero: $G_0(z)|_{z=-1}=0$ and $H_0(z)|_{z=-1}=0$. This leads to following conditions in the spatial domain

$$\begin{aligned}0=&\ \alpha\beta\gamma+\beta\gamma+[\gamma\cdot(2\alpha\beta+1)+\alpha\cdot(1+\gamma\beta)]\\&+(2\beta\gamma+1)+[\gamma\cdot(2\alpha\beta+1)+\alpha\cdot(1+\gamma\beta)]\\&+\beta\gamma+\alpha\beta\gamma\ .\end{aligned} \tag{8}$$

and

$$\begin{aligned}0=&\ \alpha\beta\gamma\delta-\beta\gamma\delta\\&+\{\delta\cdot[\gamma\cdot(2\alpha\beta+1)+\alpha\cdot(1+\gamma\beta)]+\alpha\beta\cdot(1+\gamma\delta)\}\\&-[\delta\cdot(2\beta\gamma+1)+\beta\cdot(1+\gamma\delta)]\\&+\{\alpha\cdot[\delta\cdot(2\beta\gamma+1)+\beta\cdot(1+\gamma\delta)]+(1+2\gamma\delta)+\\&\quad\alpha\cdot[\delta\cdot(2\beta\gamma+1)+\beta\cdot(1+\gamma\delta)]\}\\&-[\delta\cdot(2\beta\gamma+1)+\beta\cdot(1+\gamma\delta)]\\&+\{\delta\cdot[\gamma\cdot(2\alpha\beta+1)+\alpha\cdot(1+\gamma\beta)]+\alpha\beta\cdot(1+\gamma\delta)\}\\&-\beta\gamma\delta+\alpha\beta\gamma\delta\end{aligned} \tag{9}$$

The original aim of filter design in [4] was to create low-pass filters with frequency responses that are as flat as possible at sampling frequency by imposing a maximum number of so-called vanishing moments, i.e. multiple zeros at $H_0(z)|_{z=-1}$ and $G_0(z)|_{z=-1}$.

Multiple vanishing moments at $z=-1$ can be incorporated by substituting z with $\sqrt[n]{n^p}$ ($p=0,1,2,\ldots$) in equation (7). The second zero for $G_0(z)$ (and accordingly for $H_1(z)$ at $z=1$), for example, is included using $z=\sqrt[n]{n}$ leading to the condition

$$\begin{aligned}0=&\ 0\cdot\alpha\beta\gamma+1\cdot\beta\gamma+2\cdot[\gamma\cdot(2\alpha\beta+1)+\alpha\cdot(1+\gamma\beta)]\\&+3\cdot(2\beta\gamma+1)+4\cdot[\gamma\cdot(2\alpha\beta+1)+\alpha\cdot(1+\gamma\beta)]\\&+5\cdot\beta\gamma+6\cdot\alpha\beta\gamma\ .\end{aligned} \tag{10}$$

A different interpretation of this approach is based on the approximation of signal segments by polynomials of increasing order [8]. The condition for the second zero for $H_0(z)$ and $G_1(z)$ reads as

$$\begin{aligned}0=&\ 0\cdot\alpha\beta\gamma\delta-1\cdot\beta\gamma\delta\\&+2\cdot\{\delta\cdot[\gamma\cdot(2\alpha\beta+1)+\alpha\cdot(1+\gamma\beta)]+\alpha\beta\cdot(1+\gamma\delta)\}\\&-3\cdot[\delta\cdot(2\beta\gamma+1)+\beta\cdot(1+\gamma\delta)]+\\&4\cdot\{\alpha\cdot[\delta\cdot(2\beta\gamma+1)+\beta\cdot(1+\gamma\delta)]+(1+2\gamma\delta)+\\&\quad\alpha\cdot[\delta\cdot(2\beta\gamma+1)+\beta\cdot(1+\gamma\delta)]\}\\&-5\cdot[\delta\cdot(2\beta\gamma+1)+\beta\cdot(1+\gamma\delta)]\\&+6\cdot\{\delta\cdot[\gamma\cdot(2\alpha\beta+1)+\alpha\cdot(1+\gamma\beta)]+\alpha\beta\cdot(1+\gamma\delta)\}\\&-7\cdot\beta\gamma\delta+8\cdot\alpha\beta\gamma\delta\ .\end{aligned} \tag{11}$$

The conditions (10) and (11) are, however, not independent from (8) and (9). Two more constraints are necessary for the determination of the four weights $\alpha \ldots \delta$.

Choosing $z=\sqrt[n]{n^2}$ imposes another vanishing moment. The corresponding conditions are

$$\begin{aligned}0=&\ 0\cdot\alpha\beta\gamma+1\cdot\beta\gamma+4\cdot[\gamma\cdot(2\alpha\beta+1)+\alpha\cdot(1+\gamma\beta)]\\&+9\cdot(2\beta\gamma+1)+16\cdot[\gamma\cdot(2\alpha\beta+1)+\alpha\cdot(1+\gamma\beta)]\\&+25\cdot\beta\gamma+36\cdot\alpha\beta\gamma\ .\end{aligned} \tag{12}$$

$$\begin{aligned}0=&\ 0\cdot\alpha\beta\gamma\delta-1\cdot\beta\gamma\delta\\&+4\cdot\{\delta\cdot[\gamma\cdot(2\alpha\beta+1)+\alpha\cdot(1+\gamma\beta)]+\alpha\beta\cdot(1+\gamma\delta)\}\\&-9\cdot[\delta\cdot(2\beta\gamma+1)+\beta\cdot(1+\gamma\delta)]+\\&16\cdot\{\alpha\cdot[\delta\cdot(2\beta\gamma+1)+\beta\cdot(1+\gamma\delta)]+(1+2\gamma\delta)+\\&\quad\alpha\cdot[\delta\cdot(2\beta\gamma+1)+\beta\cdot(1+\gamma\delta)]\}\\&-25\cdot[\delta\cdot(2\beta\gamma+1)+\beta\cdot(1+\gamma\delta)]\\&+36\cdot\{\delta\cdot[\gamma\cdot(2\alpha\beta+1)+\alpha\cdot(1+\gamma\beta)]+\alpha\beta\cdot(1+\gamma\delta)\}\\&-49\cdot\beta\gamma\delta+64\cdot\alpha\beta\gamma\delta\ .\end{aligned} \tag{13}$$

Equations (10) – (13) form a system of non-linear equations resulting to the irrational weights

$$\begin{aligned}&\alpha\approx-1.58613434206 &&\gamma\approx 0.88291107553\\&\beta\approx-0.05298011857 &&\delta\approx 0.44350685204\ .\end{aligned} \tag{14}$$

Due to the inherent structure of the filter bank, each of the conditions impose double zeros, i.e. each filter shows four vanishing moments in total.

The result is exactly the same as derived from the factorisation of a polyphase matrix presented in [4].

Table 1: Parametrised design, resulting lifting weights, and results of lossless compression [bpp]

Case	α	β	γ	δ	$\tilde{N}$	N	taps	kodim07	kodim08	kodim09
0	-1/2	1/4	0	0	2	2	5/3	**3.7774**	**5.5307**	**4.0270**
1	-1	-1/4	1/3	15/16	4	2		3.8688	5.6349	4.1060
2	$-\frac{\sqrt{2}+3}{4}$	$2\cdot\sqrt{2}-3$	$\frac{2+\sqrt{2}}{8}$	$\frac{6\cdot\sqrt{2}-7}{2}$	4	2		3.8486	5.6065	4.0905
3	-5/4	-1/9	9/16	16/27	4	2		3.8660	5.5866	4.0879
4	-4/3	-9/100	25/39	$\frac{1079}{2000}$	4	2		3.8657	5.5836	4.0917
5	-3/2	-1/16	4/5	15/32	4	2		3.8467	5.5762	4.0908
6	-1.5861..	-0.05298..	0.8829..	0.4435..	**4**	**4**	9/7	3.8430	5.5729	4.0945
7	-8/5	-25/484	121/135	$\frac{9369}{21296}$	4	2		**3.8394**	5.5731	4.0935
8	-7/4	-1/25	25/24	51/125	4	2		3.8525	5.5738	4.0966
9	-17/32	$\frac{164-20\cdot\sqrt{4249}}{1089}$	$\frac{2137-5\cdot\sqrt{4249}}{65536}$	$\frac{79825+5405\cdot\sqrt{4249}}{287496}$	2	4		3.9343	5.5804	4.1399
10	-3/4	$\frac{3-2\cdot\sqrt{21}}{25}$	$\frac{11-\sqrt{21}}{32}$	$\frac{32+12\cdot\sqrt{21}}{125}$	2	4		3.8602	**5.5718**	**4.0707**
11	-1	$\frac{7-\sqrt{265}}{72}$	$\frac{29-\sqrt{265}}{32}$	$\frac{205+17\cdot\sqrt{265}}{864}$	2	4		**3.8231**	**5.5614**	**4.0574**
12	-3/2	$\frac{9-\sqrt{273}}{128}$	$\frac{23-\sqrt{273}}{8}$	$\frac{217+15\cdot\sqrt{273}}{1024}$	2	4	9/7	3.8426	5.5755	4.0878
13	-7/4	$\frac{25-4\cdot\sqrt{115}}{405}$	$\frac{70-5\cdot\sqrt{115}}{16}$	$\frac{740+76\cdot\sqrt{115}}{3645}$	2	4		3.8632	5.5783	4.1050
14	-11/4	$\frac{21-2\cdot\sqrt{237}}{507}$	$\frac{477-27\cdot\sqrt{237}}{32}$	$\frac{1188+80\cdot\sqrt{237}}{6591}$	2	4		3.9602	5.6233	4.1953

3.2 Parameterisation through relaxing constraints

Starting from the design example above and removing either the constraint (12) or the constraint (13), new filter banks with varying properties are derived. **Table 1** contains several investigated cases with different sets of lifting weights $\alpha \dots \delta$. The $\tilde{N}$ column denotes the number of vanishing moments in the analysis high-pass filter, N the number of vanishing moments in the analysis low-pass filter. The 'taps' column indicates the lengths of the corresponding analysis low-pass/high-pass filters. The last three columns contain the bitrates for lossless compression of three different grey-scale images using a JPEG2000-like compression system. The test images are taken from [12]. Only the green component for each has been used for investigations.

The first row shows the values for the 5/3 filter bank used in JPEG2000 for comparison. With respect to the processing structure depicted in Figure 2, only the two first lifting steps are activated and γ and δ are accordingly equal to zero.

Removing the constraint (13) releases one pair of zeros in $G_1(z)$ and $H_0(z)$ leading to $(\tilde{N}, N) = (4, 2)$ filter banks and a dependency of the weights on α

$$\beta = -\frac{1}{4\cdot(2\alpha+1)^2} \qquad \gamma = -\frac{4\alpha+1+4\alpha^2}{4\alpha+1}$$

$$\delta = \frac{(8\alpha^2+6\alpha+3)\cdot(4\alpha+1)}{16\cdot(2\alpha+1)\cdot(4\alpha+1+4\alpha^2)} \tag{15}$$

The released pair of zeros can now be moved in order to modify the frequency responses (cases 1 to 8 in Table 1, sorted by α). The cases 1, 3, 5, and 8 have also been found by a different design approach [11] and case 5 also by [6]. **Figure 3**a) visualises the moving zeros in $H_0(z)$. The complex pairs of zeros on the unit circle belong to cases 1 ... 5 leading to a steeper slope of the low-pass filter (**Fig. 3**b), case 6 is the original 9/7 filter with $(\tilde{N}, N) = (4, 4)$.

Keeping constraint (13) and ignoring (12) instead releases a pair of zeros in $H_1(z)$ and $G_0(z)$ leading to $(\tilde{N}, N) = (2, 4)$ filter banks. Based on the variation of α, different sets of lifting weights can be derived (Cases 9 ... 14). The complex pairs of zeros on the unit circle in **Fig. 4**a) belong to cases 13 and 14. In contrast to the (4,2)-filter banks, now the analysis high-pass filter is more affected by the parameterisation than the low-pass filter, as can be seen in **Fig. 4**b).

4 Compression results and discussion

A JPEG2000-like compression system was used for the reversible compression of three grey-scale images with typical but still different characteristics. Table 1 contains the compression results in bits per pixel indicating the superiority of the simple 5/3 filter bank. The rounding of intermediate values at each single lifting step affects the characteristic of the filters, which are no longer necessarily true low or high-pass filters. The more lifting steps that are involved, the higher the degradation of the filter properties. **Figure 5** shows

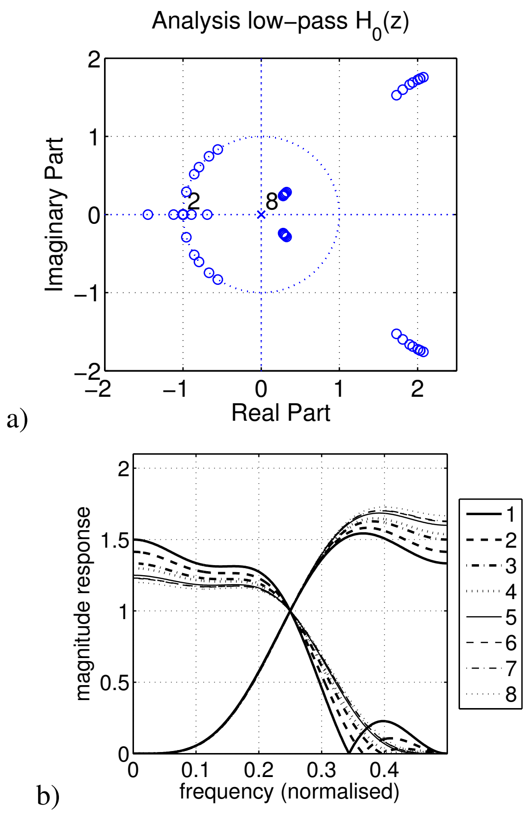

Figure 3: Cases 1 . . . 8: a) movement of the zeros of the analysis low-pass filter dependent on α, β, γ and δ; b) frequency responses of analysis filters (case 7 is almost identical to 6).

the deviation of the magnitude response (cases 0 and 6) depending on the value of a single impulse functioning as input signal. The smaller the input value the higher the effect of rounding.

The reasons for the superiority of the 5/3 filters lie in the minimal accumulated influence of rounding at each lifting step leading to a minimal change in the filter characteristics (Fig. 5a). Not only the number of steps is lower (only two instead of four in all other cases), but also the rounding error in its first step is minimal, since the factor of $\alpha = -1/2$ only leads to errors when the sum of x_{2m} and x_{2m+2} (see eq.(1), first equation) is odd. The degradation of the magnitude response of the 9/7 filter, case 6, is distinctly higher (Fig. 5b).

Comparing the compression results of cases 1 to 14, it is interesting to see that case 11 is the best 9/7 filter bank for all three test images. One reason could be the absence of rounding errors in the first lifting step ($\alpha = -1$), but this also holds true for case 1 having a distinctly worse performance. **Figure 6** shows the affected filter characteristics. It is likely that the relatively high gain of the low-pass filter of case 1 leads

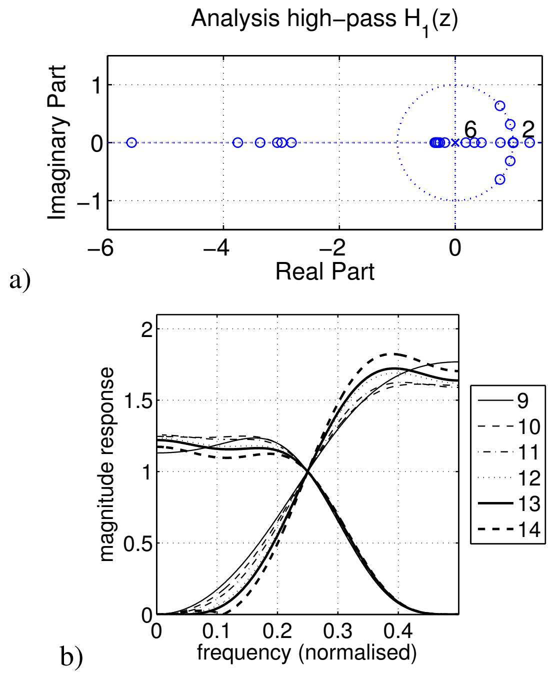

Figure 4: Cases 9 . . . 14: a) movement of the zeros of the analysis high-pass filter dependent on α, β, γ and δ; b) frequency responses of analysis filters.

to an unfavourable propagation of signal energy from one decomposition level to the next.

5 Summary

A new lifting-based method for filter design has been proposed which has the advantage of determining coefficients directly instead of factorising the known filter banks, as introduced in [5]. The method was demonstrated based on the 9/7 filter, but is applicable when designing arbitrary lifting-based filter banks. Even keeping the structure of Figure 2 and exchanging the constraints, impulse responses with different lengths can be derived, as, for example, in the 5/3 wavelet filter. The application of the newly designed filters to lossless image compression did not lead to an improvement compared to the 5/3 wavelet filter used in JPEG2000 due to disadvantageous non-linear effects of rounding. The derived filters, however, may also be applied in lossy compression systems, where rounding to integers is not required.

References:

[1] Antonini, M.; Barlaud, M.; Mathieu, P.; Daubechies, I.: Image Coding Using Wavelet Transform. *IEEE Trans. on Image Proc.*, Vol.1, No.2, April 1992, 205–220

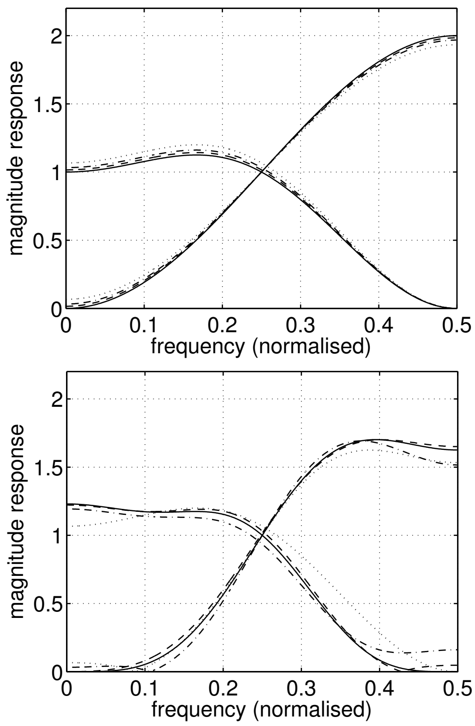

a) b)

Figure 5: Change of magnitude response caused by rounding to integer values: a) case 0; b) case 6.

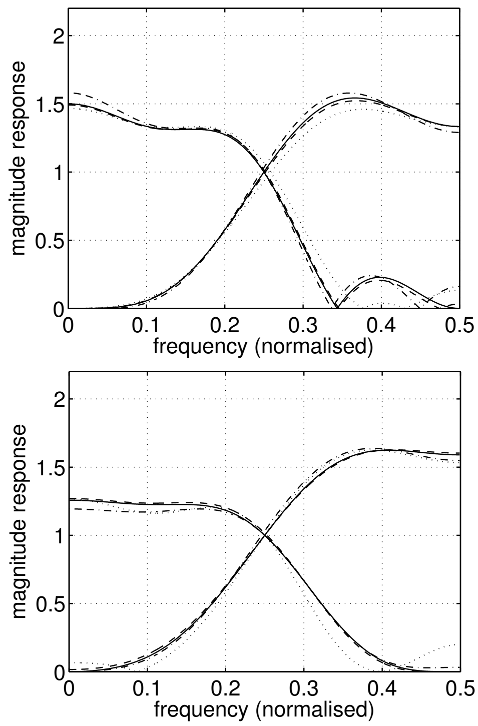

a) b)

Figure 6: Change of magnitude response caused by rounding to integer values: a) case 1; b) case 11.

(solid: transfer function without rounding; dash, dash-dot, and dot indicate signal values of 63, 31, and 15 used for determination of the impulse responses with rounding)

[2] Barua, S.; Kotteri, K.A.; Bell, A.E.; Carletta, J.E.: Optimal quantized lifting coefficients for the 9/7 wavelet. *ICASSP '04*, Vol.5, 17-21 May 2004, V–193–6

[3] Calderbank, A.R.; Daubechies, I.; Sweldens, W.; Yeo, B.L.: Wavelet transform that maps integers to integers. *Applied Computational and Harmonic Analysis*, Vol.5, No.3, 1998, 332–369

[4] Cohen, A.; Daubechies, I.; Feauveau, J.-C.: Biorthogonal Bases of Compactly Supported Wavelets. *Comm. on Pure and Applied Mathematics*, Vol.45, 1992, 485–560

[5] Daubechies, I.; Sweldens, W.: Factoring Wavelet Transform into Lifting Steps. *J. Fourier Anal. Appl.*, Vol.4, No.3, 1998, 247–269

[6] Guangjun, Z.; Lizhi, C.; Huowang, C.: A simple 9/7-tap wavelet filter based on lifting scheme. *IEEE Int. Conf. on Image Processing*, Vol.2, 2001, 249-252.

[7] ISO/IEC JTC1/SC29/WG11 N1890, *Information technology – JPEG 2000 Image Coding System*. JPEG 2000 Part I, Final Draft Intern. Standard 15444, 25 Sep.2000

[8] Strutz, T.; Müller, E.: Wavelet filter design for image compression. *IEEE-SP Int. Symposium on Time-Frequency and Time-Scale Analysis*, Paris, 18-21 June 1996, 273–276

[9] Sweldens, W.: The Lifting Scheme: A New Philosophy in Biorthogonal Wavelet Construction. *Proc. of SPIE*, Vol.2569, San Diego, USA, July 1995, 68–79

[10] Tay, D.B.H.: Rationalizing the coefficients of popular biorthogonal wavelet filters. *IEEE Trans. Circ. and Sys. for Video Techn.*, Vol.10, No.6, Sep.2000, 998–1005

[11] Tay, D.B.H.: A class of lifting based integer wavelet transform. *IEEE Int. Conf. on Image Processing*, Vol.1, 07-10 Oct. 2001, Thessaloniki, Greece, 602–605

[12] http://r0k.us/graphics/kodak/, Oct. 2008